Rare Met.
https://doi.org/10.1007/s12598-023-02559-8

RARE METALS

LETTER

Creep rupture life predictions for Ni-based single crystal superalloys with automated machine learning

Chang-Lu Zhou, Rui-Hao Yuan*, Wei-Jie Liao, Ting-Huan Yuan, Jiang-Kun Fan, Bin Tang, Ping-Xiang Zhang, Jin-Shan Li*, Turab Lookman

Received: 12 April 2023 / Revised: 22 May 2023 / Accepted: 12 June 2023

The state of the art for data-driven creep rupture life predictions incorporates microstructural and deformation characteristics into machine learning. However, the microstructures and deformation mechanisms for unknown alloys are inaccessible and uncertain before experiments are carried out, and therefore prevents extrapolations of the learned models. We report a simplified but accurate and generalizable surrogate model for creep rupture life predictions for Ni-based single crystal superalloys using an automated machine learning algorithm implemented in Autogluon. Without incorporating microstructural information or deformation mechanisms into the machine learning framework, we demonstrate that prediction accuracies of creep rupture life can be improved on independent test data. The obviation of the incorporation of microstructures and deformation mechanism with machine learning not only makes the surrogate model readily applicable to a vast unexplored composition/processing space, but also facilitates the efficient inverse design of new alloys. Our work shows that automated machine learning software creates surrogate models with minimum human intervention, showing promise in the design of superalloys.

Nickel-based superalloys that possess excellent high temperature strength, good oxidation resistance, fatigue resistance [1] and creep resistance [2] are key structural components in aerospace applications such as aero-engine blades, turbine disks and combustion chambers [3]. The creep rupture life characterizing creep resistance, which largely depends on the compositions, processing parameters, experimental conditions, and microstructures of the alloys, is one of the central indicators for high temperature applications [4]. However, the harsh service environment and long period nature make the measurement of creep rupture lifetime rather time-consuming and costly [5]. Therefore, there is a need for accurate predictions of creep rupture life from compositions, processing parameters, experimental conditions, and microstructures. These could alleviate expensive experimental work and even facilitate the design of new alloys via inverse inference [6–8].

Extensive effort has been devoted to the development of prediction methods, for example, via empirical, theory-based models and machine learning (ML)-driven surrogate models [9–12]. Traditionally, the empirical and theory-based methods include approaches based on time–temperature parameters (TTP) and creep constitutive models (CCM). The former only has two variables, i.e., the applied stress and measured temperature, and a group of measurements with different stress and temperature need to be conducted to fit the coefficients in the TTP models for further extrapolation [10, 13]. The latter utilizes various microscopic parameters such as the rate of dissipation and reduced energy dissipation as inputs to construct CCM

Supplementary Information The online version contains supplementary material available at https://doi.org/10.1007/s12598-023-02559-8.

C.-L. Zhou, R.-H. Yuan*, W.-J. Liao, T.-H. Yuan, J.-K. Fan, B. Tang, P.-X. Zhang, J.-S. Li*
State Key Laboratory of Solidification Processing, Northwestern Polytechnical University, Xi'an 710072, China
e-mail: rhyuan@nwpu.edu.cn

J.-S. Li
e-mail: ljsh@nwpu.edu.cn

R.-H. Yuan
Chongqing Innovation Center, Northwestern Polytechnical University, Chongqing 401120, China

T. Lookman
AiMaterials Research LLC, Santa Fe, NM 87501, USA

Published online: 27 February 2024

models for creep rupture life [9, 14, 15]. These two kinds of models are usually developed for specific alloy systems and could be extrapolated to the long-term creep rupture life prediction, as well as provide physical insights for the creep behavior. However, there are still sizeable deviations between model predictions and measurements [16, 17]. Furthermore, they are limited in scope if new compositions are considered as the one-to-one mapping from composition to the property is lacking [18].

Recently, ML has been applied in materials science to accelerate materials discoveries [19–21]. A number of studies have made ML-based predictions of creep behavior for structural materials [11, 12]. In general, ML learns the mapping from inputs to outputs, where the inputs are usually compositions, processing parameters, experimental conditions, and microstructural characteristics, whereas the outputs are the properties concerned, such as the creep rupture lifetime herein. That is, a direct composition-processing-structure–property can be established in principle for both prediction and inverse design. More importantly, in contrast to traditional empirical and theory-based strategies, ML is capable of considering a full set of multiscale information simultaneously and thus has the potential to improve the prediction accuracy of creep rupture lifetime [22].

In the ML-driven studies for prediction of creep rupture lifetime, the state of the art is to take into account the various microstructures and deformation mechanisms of different alloys when building the mapping, $y = f(x)$, to obtain an improved predictive surrogate model [23, 24]. For example, by introducing high throughput calculated microstructures as inputs, Shin et al. [23] established qualified ML-based surrogate models for creep rupture life of iron-based high temperature superalloys. In addition to microstructures, it is believed that the mechanical deformation mechanism at high temperatures is quite different for various alloys. Thus, it is thought that the appropriate formulation of different deformation mechanisms and their incorporation into ML might enhance the robustness of the surrogate models for creep rupture life. Guided by this, Liu et al. [24] proposed a divide-and-conquer approach (DCSA) and demonstrated its efficacy in the prediction of creep rupture life of Ni-based single crystal superalloys. The alloys with diverse deformation mechanisms were first clustered into different groups, and then for each group, the algorithms with the best fitting performance are selected for prediction. However, even though the coefficient of determination (R^2) of the learned surrogate models is claimed to be as high as 0.91 in the training data, the model performance degenerated severely ($R^2 \sim 0.79$) when extrapolating to an independent test data (Fig. 1a). This suggests that the DCSA method based on microstructures and deformation mechanisms is sensitive to the different types of alloys.

In the present study, we propose to obtain a simplified but accurate ML-based prediction of the creep rupture life of Ni-based single crystal alloys. By using the integration in Autogluon of classical ML algorithms such as random forest and gradient boosting trees, we show that R^2 of the learned surrogate model on independent test data is improved from 0.79 (DSCA) to 0.92 (our method), with an enhancement as high as 16%. The much-improved accuracy and generalizability are obtained without employing microstructural and deformation characteristics, which are often not accessible and uncertain for new alloys before experiments (Fig. 1b).

The Ni-based single crystal superalloys dataset used has been published in Ref. [24], which was derived from 14 published patents. The dataset includes 266 alloys that were tested under four conditions, i.e., high temperature and low stress, high temperature and high stress, low temperature and low stress, and low temperature and high stress. There are in total 27 features [24] that have been categorized into four types to describe the targeted creep rupture lifetime. Specifically, they are 14 chemical compositions, 6 heat treatment processing parameters, 2 test conditions, and 5 microstructural features from thermodynamic calculations (the mole fraction of γ' precipitates, diffusion coefficient of alloying elements inside γ phase, and shear modulus, weighted average lattice parameter and stacking fault energy of the alloy). We analyze the distribution of both the 27 features and creep rupture lifetime in Fig. S1. It is shown that the data are biased to some certain value. To evaluate the generalizability of the surrogate model, other eight Ni-based single crystal superalloys with very different chemical compositions were also collected from four published patents [25–28].

Following Ref. [24], the features are processed with the max–min normalization to eliminate the possible influence of different dimensions on the ML model. In addition, the output (y) of the ML model finally used is the ln(creep rupture life), i.e., y = ln(creep rupture life). The automated ML model (Autogluon [29]) adopted in this study combines different algorithms, such as XGBoost [30], LightGBM [31], CatBoost [32], RF [33], extra-trees [34] and k-nearest neighbors [35]. Compared to single models, the automated model takes advantage of different models to enhance the prediction. There are three key elements incorporated in Autogluon. The first is stacking, where each single model is trained using the initial dataset and the final prediction is obtained using the sum of the outputs from each model by considering the trained weight. The second is the use of a bagging strategy to avoid possible over-fitting especially when the dataset is sparse. The last is multi-layer stacking.

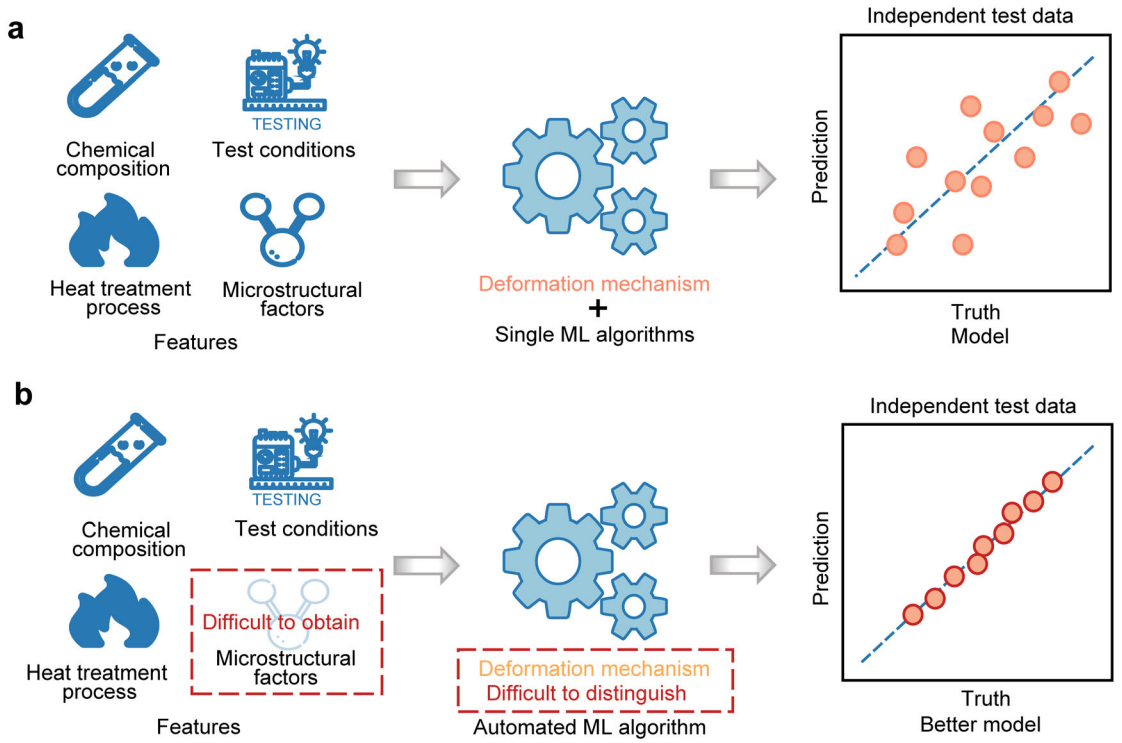

Fig. 1 **a** Prediction of creep rupture life by incorporating microstructures and deformation mechanism into ML framework; **b** improved ML model without taking into account inaccessible and uncertain microstructures and deformation mechanism

It feeds the output of the prediction by the stacker models as inputs to additional higher-layer stacker models. Taking the 2-layer stacking as an example, the output of the first layer is used as a feature, then combined with the initial features to retrain the ML model. For the 3-layer stacking, the output from the 2-layer stacking is integrated with the initial features to build the ML model. This procedure is repeated for more stacking layers. The hyper-parameters, that is, the number of stacking layers and bagging, are optimized using grid search.

The initial 266 alloys are randomly divided into a training set and a test set in 9:1. The former is used to train the model, and the latter validates the model's performance. To obtain statistically meaningful results, the initial dataset is randomly divided 50 times and the errors/accuracies of different models are averaged for the final error/accuracy. Five single regression models, random forest (RF), support vector regression (SVR), Gaussian process regression (GPR), lasso regression (LR) and ridge regression (RR), are trained for comparison, and the corresponding hyper-parameters are optimized using the grid search together with cross-validation.

Three commonly employed statistical indicators are used to evaluate the model performance, i.e., mean absolute percentage error (MAPE), mean square error (MSE), and R^2. These are defined by:

$$\mathrm{MAPE} = \frac{100\%}{n}\sum_{i=1}^{n}\left|\frac{\hat{y}_i - y_i}{y_i}\right| \tag{1}$$

$$\mathrm{MSE} = \frac{1}{n}\sum_{i=1}^{n}(y_i - \hat{y}_i)^2 \tag{2}$$

$$R^2 = 1 - \frac{\sum_{i=1}^{n}(y_i - \hat{y}_i)^2}{\sum_{i=1}^{n}(y_i - \bar{y})^2} \tag{3}$$

where y_i and $\hat{y}_i$ indicate the actual and predicted values, respectively. $\bar{y}$ is the mean of y_i and n is the number of samples in the dataset.

We first employ five commonly used algorithms to learn the relationship between 27 features and creep rupture life. For simplicity, only the performance of the SVR model is shown in Fig. 2a, which is consistent with that reported in Ref. [24]. The SVR model does not perform particularly well, given the large deviation of the training (blue) and test (yellow) points in the diagonal plot. To allow comparison, the result from DCSA is reproduced in Fig. 2b. The predictions, especially for long-term creep, are improved. However, it should be noted that in the reproduced Fig. 2b, all the 266 samples were used as training data. Thus, its generalizability should be further evaluated.

Figure 2c is a plot of the results from the automated ML model. For both training and test data, the samples

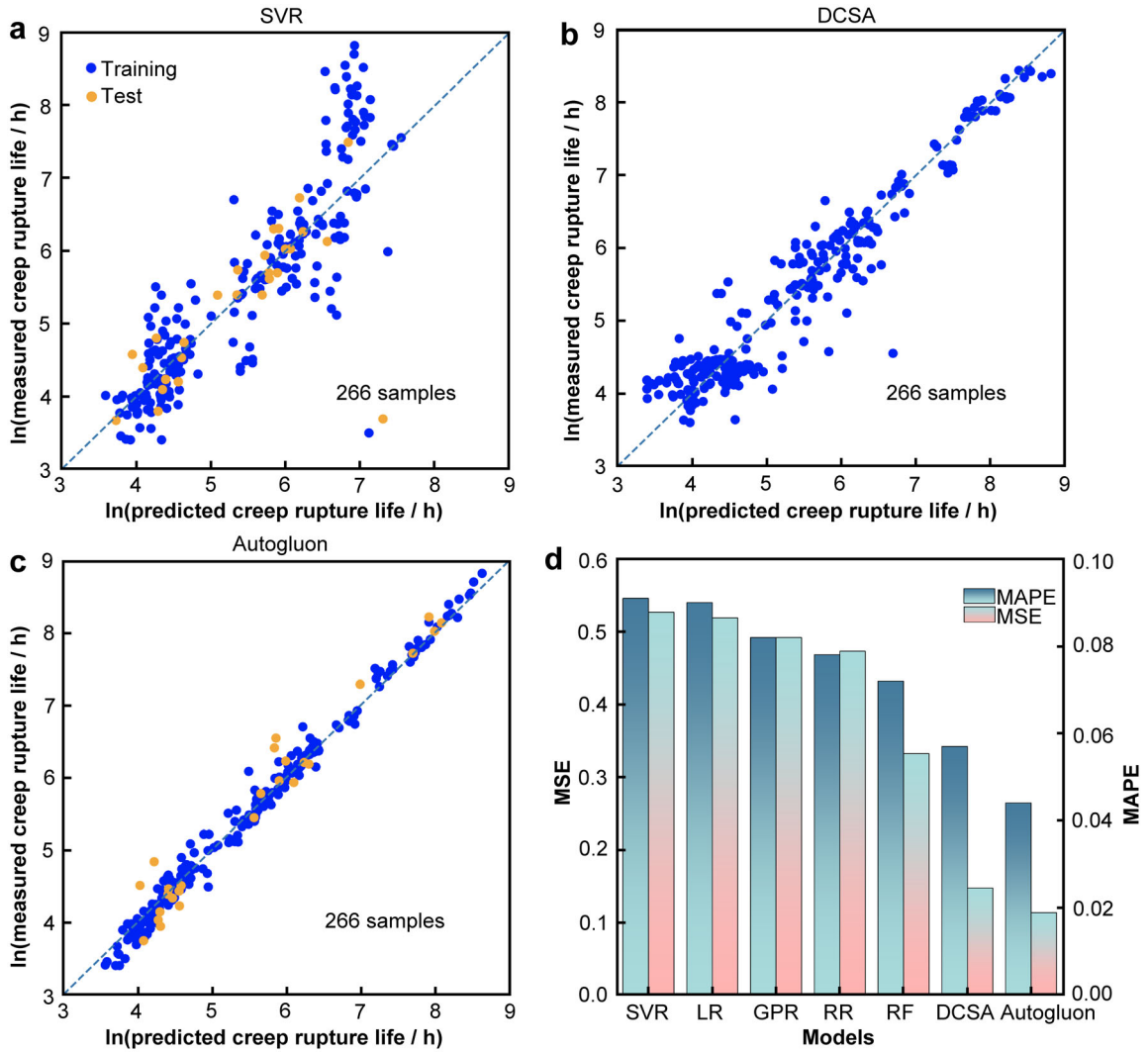

Fig. 2 Comparing performance of different models on 266 creep data: **a** single model; **b** model combining deformation mechanism; **c** automated model without deformation mechanism; **d** MAPE and MSE for each model

distribute well about the diagonal line, indicating the robustness of the automated model for Ni-based single crystal superalloys. Figure 2d compares the performance of five single models, and the results from DCSA and Autogluon. The two errors, i.e., MAPE and MSE for the five single models and Autogluon are estimated by considering 50 randomly divided test data. The two errors for DCSA are obtained using all the 266 samples for the training data, and there is a clear tendency that the errors decrease monotonously from left to right, suggesting that Autogluon performs the best consistently. Thus, without considering the complicated deformation mechanism, we are able to capture the principal tendencies underlying the superalloy data. The circumvention of complicated and uncertain deformation mechanisms not only simplifies the procedures for training the ML model, but also improves the resultant accuracy.

We next validate the generalizability of the trained models by comparing predictions of 8 quite independent Ni-based single crystal superalloys, which have very different chemical compositions and measured conditions compared to the initial 266 alloys. Thus, in total we have 274 samples. Following the same process, the models are retrained and plotted in Fig. 3 where 8 independent samples are represented by red triangles. Specifically, Fig. 3a shows the result from the DCSA method (reproduced from Ref. [24]), and the model performance degenerates for samples with high creep rupture life. This suggests that DCSA learned in Fig. 2b possesses relatively poor generalizability. In contrast, the Autogluon-based model performs much better using the 274 samples (Fig. 3b), with R^2 improving from $\sim$0.79 to $\sim$0.92, indicating that this model can be used for independent samples. It should be noted that the Autogluon model performs a little better on

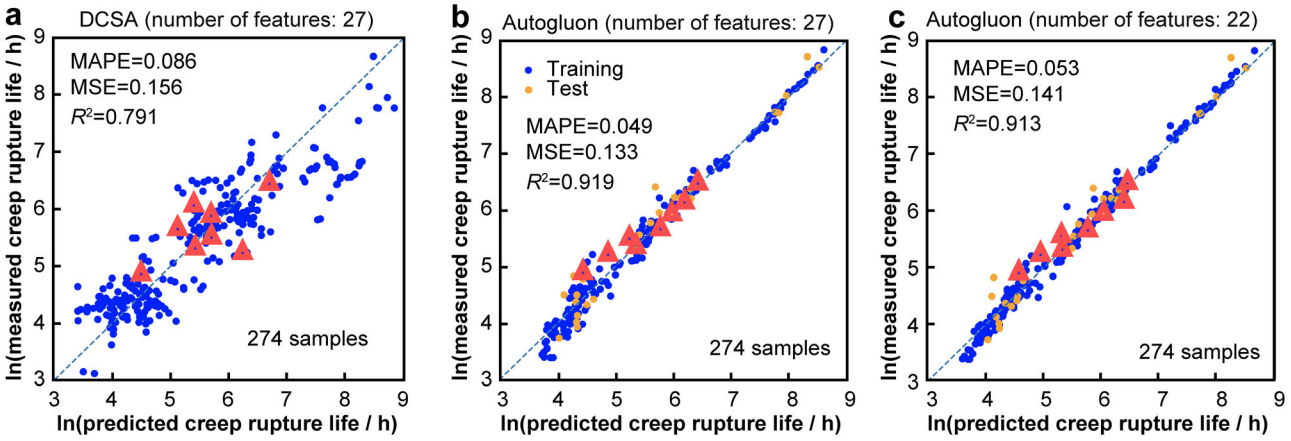

Fig. 3 Generalizability of trained models on 8 independent samples (red triangles). **a** Model with both deformation mechanism and microstructures; **b** automated model without deformation mechanism; **c** automated model without both deformation mechanism and microstructures

the alloys with long-term creep life, compared to the ones with short-term creep life. The possible origin might lie on the number of alloys with long-term creep life, which is much less than the alloys with short-term creep life. The imbalanced data could lead to bias in the ML model.

In the analysis above, all the 27 features including compositions, processing parameters, testing conditions, and microstructures have been used to train the ML model. Even the microstructure plays an important role in the creep behavior, however, it has two drawbacks when predicting the creep behavior of unknown alloys. (1) The comprehensive quantification of microstructures is challenging, for example, the size, shape and distribution of precipitates that can strengthen the alloys [36]. (2) The microstructures for plenty of unknown alloys are inaccessible unless the accurate and cheap multi-scale high throughput calculations are realizable. Therefore, we naturally wonder how the model behaves if the microstructures are absent in the features. Figure 3c shows the performance of the automated model based on Autogluon, where the five microstructural parameters are not used to train the model. Intriguingly, the surrogate model behaves similarly to Fig. 3b, indicating the robustness of the automated ML model. Thus, it can be concluded that the surrogate model is further simplified without sacrificing accuracy, by obviating the use of microstructures as inputs.

To gain insight into the influence of microstructures on the ML-based surrogate model, we ranked the features using Autogluon by considering their effect on model error. Figure 4 shows that heat treatment processing parameters, including aging treatment temperature and time, play important roles in the prediction of creep rupture life. The next two parameters are the testing conditions, that is, the testing temperature and applied stress. It is interesting to see that the 2nd step aging time ranks higher than the 2nd step aging temperature. The possible origins can be attributed to the data distribution of these two parameters. As shown in Fig. S1o and r, the aging time distributes more discretely than aging temperature. It will rank higher when building the ML model because it encodes more information. In addition, we found two elements, e.g., Cr and Re rank the top two among all the elements. This is consistent with previous studies, which have shown that Cr can increase the volume fraction of γ' phase [37], while Re can strengthen the γ phase and the γ/γ' interface of Ni-based superalloys [38, 39]. These effects finally benefit the creep life. Although creep behavior depends largely on microstructure [40, 41], the five microstructural parameters rank relatively low, as highlighted by dark blue in Fig. 4. The possible origins can be ascribed to two aspects: insufficient microstructural information and the data distribution, as will be detailed below. For simplicity, we use the volume friction of γ' phase as an example. Firstly, the microstructures, embody multi-scale information ranging from atomistic, mesoscopic and macroscopic scales. It is thus quite complex and difficult to distinguish which descriptors dominate. Here, the five thermodynamically and phenomenologically calculated parameters may not be adequate to capture the full microstructural information. The other parameters from different length scales, e.g., the morphology and distribution of γ' precipitates that could have crucial effects on the creep behavior are not included. We thus recognize that it is essential to incorporate efficient and comprehensive digital representations of microstructures for improved predictions and understanding of creep behavior. Secondly, the volume fraction of γ' phase distributes in a very narrow range of 30%–40% (Fig. S2). When building ML model, it is well accepted that the features with low variance often convey poor information. As a result, these features contribute little to

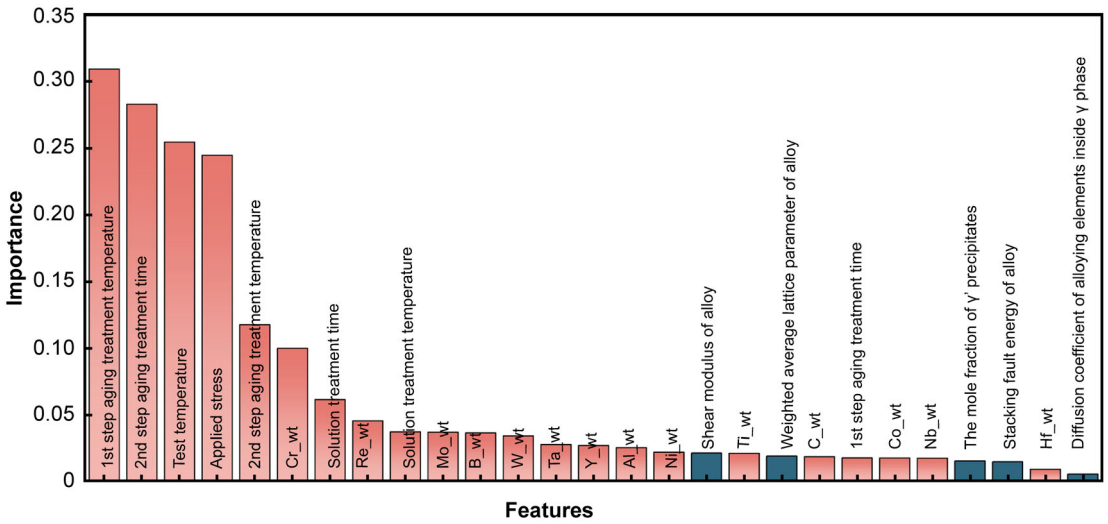

Fig. 4 Relative importance of initial 27 features ranked by automated algorithm

the model and thus rank at the end. In this work, it is able to construct a reasonable surrogate model based on the assumption that the full multi-scale microstructures are largely the result of both chemical compositions and processing conditions [42].

At the end, we try to suggest some alloys with enhanced creep rupture lifetime using the trained Autogluon model. Alloys behave well at 900 °C and 800 MPa are selected. By varying the composition and processing, we generate 1,000,000 candidates. Based on the predictions, we recommend 5 alloys that can have improved creep rupture lifetime at given test conditions, as shown in Table S1.

In summary, how a simplified but robust surrogate model can be constructed for creep rupture life of Ni-based single crystal superalloys using an automated machine learning model such as Autogluon has been demonstrated. The model uses easily accessible chemical compositions, processing parameters, and test conditions as inputs. More importantly, compared to the state-of-the-art surrogate models that combine microstructures and deformation mechanisms, our model improves the prediction accuracy, e.g., the R^2 increases from 0.79 to 0.92 for an independent test data set. The model circumvents the need for inaccessible microstructures and uncertain deformation mechanisms of unknown alloys and requires merely composition and processing data, which are more readily available for design.

Acknowledgements This study was financially supported by the National Key Research and Development Program of China (No. 2021YFB3702601), the National Science and Technology Major Project of China (No. J2019-VI-0023-0140), the National Natural Science Foundation of China (No. 52002326) and the Natural Science Foundation of Chongqing (No. cstc2021jcyj-msxmX0602).

Declarations

Conflict of interests The authors declare that they have no conflict of interest.

References

[1] Feng WH, Chang JX, Zhu SD. Nickel-based single crystal superalloys with different rhenium contents. Rare Met. 2021; 45(3):353. https://doi.org/10.1373/j.cnki.cjrm.XY20050020.
[2] Tian SG, Su Y, Qian BJ, Yu XF, Liang FS, Li AA. Creep behavior of a single crystal nickel-based superalloy containing 4. 2% Re. Mater Des. 2012;37:236. https://doi.org/10.1016/j.matdes.2012.01.008.
[3] Zhang XS, Chen YZ, Hu JL. Recent advances in the development of aerospace materials. Prog Aerosp Sci. 2018;97:22. https://doi.org/10.1016/j.paerosci.2018.01.001.
[4] Zhang W, Wang XW, Chen HF, Zhang TY, Gong JM. Evaluation of the effect of various prior creep-fatigue interaction damages on subsequent tensile and creep properties of 9% Cr steel. Int J Fatigue. 2019;125:440. https://doi.org/10.1016/j.ijfatigue.2019.04.018.
[5] Cui LQ, Yu JJ, Liu JL, Jin T, Sun XF. The creep deformation mechanisms of a newly designed nickel-base superalloy. Mat Sci Eng A. 2018;710:309. https://doi.org/10.1016/j.msea.2017.11.002.
[6] Coakley J, Dye D, Basoalto H. Creep and creep modelling of a multimodal nickel-base superalloy. Acta mater. 2011;59(3):854. https://doi.org/10.1016/j.actamat.2010.08.035.
[7] Zhang JW, Wang GZ, Xuan FZ, Tu ST. The influence of stress-regime dependent creep model and ductility in the prediction of creep crack growth rate in Cr–Mo–V steel. Mater Des. 2015;65:644. https://doi.org/10.1016/j.matdes.2014.09.070.
[8] Kim YK, Kim D, Kim HK, Oh CS, Lee BJ. An intermediate temperature creep model for Ni-based superalloys. Int J Plast. 2016;79:153. https://doi.org/10.1016/j.ijplas.2015.12.008.

[9] Prasad SC, Rao IJ, Rajagopal KR. A continuum model for the creep of single crystal nickel-base superalloys. Acta Mater. 2005;53(3):669. https://doi.org/10.1016/j.actamat.2004.10.020.
[10] Kim WG, Yin SN, Lee GG, Kim YW, Kim SJ. Creep oxidation behaviour and creep strength prediction for alloy 617. Int J Pres Ves Pip. 2010;87(6):289. https://doi.org/10.1016/j.ijpvp.2010.03.008.
[11] Wang JQ, Fa YZ, Tian Y, Yu XH. A machine-learning approach to predict creep properties of Cr–Mo steel with time-temperature parameters. J Mater Res Technol. 2021;13:635. https://doi.org/10.1016/j.jmrt.2021.04.079.
[12] Wang CC, Wei XL, Ren D, Wang X, Xu W. High-throughput map design of creep life in low-alloy steels by integrating machine learning with a genetic algorithm. Mater Design. 2022;213: 110326. https://doi.org/10.1016/j.matdes.2021.110326.
[13] Tamura M, Abe F, Shiba K, Sakasegawa H, Tanigawa H. Larson-Miller constant of heat-resistant steel. Metall Mater Trans A. 2013;44(6):2645. https://doi.org/10.1007/s11661-013-1631-0.
[14] Hore S, Ghosh RN. Computer simulation of the high temperature creep behaviour of Cr–Mo steels. Mat Sci Eng A. 2011;528(19–20):6095. https://doi.org/10.1007/s11661-013-1631-0.
[15] Meng QH, Wang ZQ. Creep damage models and their applications for crack growth analysis in pipes: a review. Eng Fract Mech. 2019;205:547. https://doi.org/10.1016/j.engfracmech.2015.09.055.
[16] Vladimirov IN, Reese S, Eggeler G. Constitutive modelling of the anisotropic creep behaviour of nickel-base single crystal superalloys. Int J Mech Sci. 2009;51(4):305. https://doi.org/10.1016/j.ijmecsci.2009.02.004.
[17] Dang YY, Zhao XB, Yuan Y, Ying HF, Lu JT, Yang Z, Gu Y. Predicting long-term creep-rupture property of inconel 740 and 740H. Mater High Temp. 2016;33(1):1. https://doi.org/10.1179/1878641315Y.0000000010.
[18] MacLachlan DW, Knowles DM. Modelling and prediction of the stress rupture behaviour of single crystal superalloys. Mat Sci Eng A. 2001;302(2):275. https://doi.org/10.1016/S0921-5093(00)01829-3.
[19] Ramprasad R, Batra R, Pilania G, Mannodi-Kanakkithodi A, Kim C. Machine learning in materials informatics: recent applications and prospects. Npj Comput Mater. 2017;3(1):1. https://doi.org/10.1038/s41524-017-0056-5.
[20] Wang XY, Wang JJ, Zhang CJ, Tong WW, Jiang B, Lu GX, Wen ZX, Feng T. Creep prediction model for nickel-based single-crystal superalloys considering precipitation of TCP phase. Rare Met. 2021;40(10):2892. https://doi.org/10.1007/s12598-020-01670-4.
[21] Lookman T, Balachandran PV, Xue DZ, Yuan RH. Active learning in materials science with emphasis on adaptive sampling using uncertainties for targeted design. Npj Comput Mater. 2019;5(1):1. https://doi.org/10.1038/s41524-019-0153-8.
[22] Biswas S, Castellanos DF, Zaiser M. Prediction of creep failure time using machine learning. Sci Rep. 2020;10(1):1. https://doi.org/10.1038/s41598-020-72969-6.
[23] Shin D, Yamamoto Y, Brady MP, Lee S, Haynes JA. Modern data analytics approach to predict creep of high-temperature alloys. Acta Mater. 2019;168:321. https://doi.org/10.1016/j.actamat.2019.02.017.
[24] Liu Y, Wu JM, Wang ZC, Lu XG, Avdeev M, Shi SQ, Wang CY, Yu T. Predicting creep rupture life of Ni-based single crystal superalloys using divide-and-conquer approach based machine learning. Acta Mater. 2020;195:454. https://doi.org/10.1016/j.actamat.2020.05.001.
[25] Schweizer FA. Single crystal nickel-base super alloy, August 23 1988. US Patent 4,765,850.
[26] Tamaki H, Yoshinari A, Okayama A, Kobayashi M, Kageyama K, Ohno T. High strength Ni-base superalloy for directionally solidified castings, April 18 2000. US Patent 6,051,083.
[27] Naik SK. High strength nickel base single crystal alloys, December 5 1989. US Patent 4,885,216.
[28] Kobayashi T, Koizumi Y, Yokokawa T, Osawa M, Harada H, Maruko T. Development of 4th generation SC Superalloys without Re. J Jpn I Met. 2005;69(2):272. https://doi.org/10.2320/jinstmet.69.272.
[29] Erickson N, Mueller J, Shirkov A, Zhang H, Larroy P, Li M, Smola A. Autogluon-tabular: robust and accurate automl for structured data. arXiv preprint 2020. https://doi.org/10.48550/arXiv.2003.06505.
[30] Chen TQ, He T, Benesty M, Khotilovich V, Tang Y, Cho H, Chen KL, Mitchell R, Cano I, Zhou T. Xgboost: extreme gradient boosting. R packag vers 04–2. 2015;1(4):1.
[31] Ke GL, Meng Q, Finley T, Wang TF, Chen W, Ma WD, Ye QW, Liu TY. Lightgbm: a highly efficient gradient boosting decision tree. Adv. Neural Inf. Process. Syst. 2017;30. https://github.com/Microsoft/LightGBM.
[32] Prokhorenkova L, Gusev G, Vorobev A, Dorogush AV, Gulin A. Catboost: unbiased boosting with categorical features. Adv. Neural Inf. Process. Syst. 2018;31. https://github.com/catboost/catboost.
[33] Breiman L. Random forests. Mach Learn. 2001;45(1):5. https://doi.org/10.1023/A:1010933404324.
[34] Geurts P, Ernst D, Wehenkel L. Extremely randomized trees. Mach Learn. 2006;63(1):3. https://doi.org/10.1007/s10994-006-6226-1.
[35] Peterson LE. K-nearest neighbor. Scholarpedia. 2009;4(2):1883. https://doi.org/10.4249/scholarpedia.1883.
[36] Sun JY, Wei LL, Li QS, Gong SK, Guo HB. Microstructure stability of $\gamma'+\beta$ Ni–Al coated single-crystal superalloy N5 annealed at 1100°C. Rare Met. 2021;40(3):693. https://doi.org/10.1007/s12598-017-0954-1.
[37] Chen JY, Feng Q, Cao LM, Sun ZQ. Improvement of stress–rupture property by Cr addition in Ni-based single crystal superalloys. Mat Sci Eng A. 2011;528(10–11):3791. https://doi.org/10.1016/j.msea.2011.01.060.
[38] Wu XX, Makineni SK, Liebscher CH, Dehm G, Mianroodi JR, Shanthraj P, Svendsen B, Burger D, Eggeler G, Raabe D, Gault B. Unveiling the Re effect in Ni-based single crystal superalloys. Nat Commun. 2020;11(1):389. https://doi.org/10.1038/s41467-019-14062-9.
[39] Lu F, Antonov S, Lu S, Zhang JC, Li LF, Wang D, Zhang J, Feng Q. Unveiling the Re effect on long-term coarsening behaviors of γ' precipitates in Ni-based single crystal superalloys. Acta Mater. 2022;233:117979. https://doi.org/10.1016/j.actamat.2022.117979.
[40] Kim IS, Choi BG, Jung JE, Do J, Seok WY, Lee YH, Jeong IY. Effect of heat treatment on microstructural evolution and creep behaviors of a conventionally cast nickel-based superalloy. Mater Charact. 2020;165:110378. https://doi.org/10.1016/j.matchar.2020.110378.
[41] Huang YS, Wang XG, Cui CY, Li JG, Ye LH, Hou GC, Yang YH, Liu JL, Liu JD, Zhou YZ, Sun XF. The effect of coarsening of γ' precipitate on creep properties of Ni-based single crystal superalloys during long-term aging. Mat Sci Eng A. 2020;773:138886. https://doi.org/10.1016/j.msea.2019.138886.
[42] Li Y, Chen K, Narayan RL, Ramamurty U, Wang YD, Long JC, Tamura N, Zhou X. Multi-scale microstructural investigation of a laser 3D printed Ni-based superalloy. Addit Manuf. 2020;34:101220. https://doi.org/10.1016/j.addma.2020.101220.